ARTICLE

Biomimetic Chemosensor: Designing Peptide Recognition Elements for Surface Functionalization of Carbon Nanotube Field Effect Transistors

Zhifeng Kuang, Sang N. Kim, Wendy J. Crookes-Goodson, Barry L. Farmer, and Rajesh R. Naik*

Materials and Manufacturing Directorate, Air Force Research Laboratory, Wright-Patterson AFB, Ohio 45433

ABSTRACT Single-wall carbon nanotube field effect transistors (SWNT-FETs) are ideal candidates for fabricating sensors due to their unique electronic properties and have been widely investigated for chemical and biological sensing applications. The lack of selectivity of SWNT-FETs has prompted extensive research on developing ligands that exhibit specific binding as selective surface coating for SWNTs. Herein we describe the rational design of a peptide recognition element (PRE) that is capable of noncovalently attaching to SWNTs as well as binding to trinitrotoluene (TNT). The PRE contains two domains, a TNT binding domain derived from the binding pocket of the honeybee odor binding protein ASP1, and a SWNT binding domain previously identified from the phage peptide display library. The PRE structure in the presence of SWNT was investigated by performing classical all-atom molecular dynamics simulations, circular dichroism spectroscopy, and atomic force microscopy. Both computational and experimental analyses demonstrate that the peptide retains two functional domains for SWNT and TNT binding. The binding motif of the peptide to SWNT and to TNT was revealed from interaction energy calculations by molecular dynamics simulations. The potential application of the peptide for the detection of TNT is theoretically predicted and experimentally validated using a SWNT-FET sensor functionalized with a designer PRE. Results from this study demonstrate the creation of chemosensors using designed PRE as selective surface coatings for targeted analytes.

KEYWORDS: SWNT-FETs · CNT · peptides · TNT · nanotube transistors · sensors · phage display

The unique electronic and mechanical properties of carbon nanotubes (CNTs) can be exploited for creating highly sensitive, lightweight sensors for the detection of chemical and biological agents.[1−3] The extreme sensitivity of SWNTs to molecular adsorption and changes in local environment make them attractive as sensing elements. However, SWNTs alone demonstrate low selectivity toward specified targets. For example, even the contact with an inert gas causes a change in the conductivity of SWNTs.[2] There is a need to develop surface functionalization coatings (recognition elements) for the development of selective SWNT sensors. The selective binding of a target, *via* the immobilized recognition element, onto the SWNT surface results in a selective change in electronic properties of the SWNT-FET device.[4] Due to their highly specific recognition abilities, the use of biomolecular coatings is an attractive solution for designing molecular recognition elements that can be immobilized onto the SWNT surface. Biomolecules have been used in the surface functionalization of SWNTs for various sensing applications.[2−5] For optimal performance, the immobilized biomolecules should maintain their ability to bind target analytes. Small molecules such as peptides or nucleic acid based aptamers are exceptional candidates for such applications and exhibit enhanced stability relative to large biomolecules, such as antibodies. Short peptide sequences have been covalently functionalized to silicon nanowires as selective sensors against acetic acid and ammonia.[5] Molecular templates such as peptides or aptamers that selectively bind to a given target can be identified using combinatorial approaches. Peptide sequences that are capable of binding to carbon nanotubes, metal surfaces, bacterial spores, and explosives have been previously identified from peptide libraries.[6−8]

We previously identified SWNT binding peptides by screening a combinatorial phage display peptide library.[7] The SWNT binding peptide P1 (His-Ser-Ser-Tyr-Trp-Tyr-Ala-Phe-Asn-Asn-Lys-Thr) was found to bind and disperse SWNTs. The P1 peptide was then incorporated into a bifunctional peptide (P1-R5) that was used to functionalize the surface of SWNTs with metal oxides. The P1-R5 peptide was capable of noncovalent binding to the SWNT surface *via* the P1 peptide domain and templating the growth of metal oxides on the nanotube surface *via* the R5 domain (Ser-Ser-Lys-Lys-Ser-Gly-Ser-Tyr-

*Address correspondence to rajesh.naik@wpafb.af.mil.

Received for review October 5, 2009 and accepted December 14, 2009.

Published online December 28, 2009. 10.1021/nn901365g

Ser-Gly-Ser-Lys-Gly-Ser-Lys-Arg-Arg-Ile-Leu-).[7,9] This earlier work demonstrated that biomolecular templates can be designed to impart specific functionalities to the SWNT surface. In this study, we explore the possibility of designing a short peptide recognition element (PRE) capable of binding to a target that is immobilized onto the surface of SWNT *via* the P1 peptide for the development of a SWNT-FET sensor for trinitrotoluene (TNT). One of the basic design requirements was to use a short peptide that is capable of binding to a target of choice to act as our molecular recognition element or receptor-like moiety. This peptide sequence can then be fused to the P1 peptide to create a multifunctional peptide that is capable of both binding to the SWNT surface and detecting a target molecule. Short peptide sequences have been used to develop selective SWNT-FET sensors for metal ion sensing.[3] The authors used an electropolymerization method for depositing the peptides onto the SWNT surface for detecting Ni^{2+} and Cu^{2+}. Selective detection of metal ions in the pico- to micromolar range was achieved in their study and opened up the possibilities of using selective peptide sequences for tuning the selectivity of SWNT-FETs.

In insects, odor sensing occurs in the antenna. Small proteins called odorant binding proteins (OBPs) bind and ferry hydrophobic odorant molecules from the external environment to receptors on the antennal olfactory sensilla.[10,11] The exceptional ability of insects to detect chemical signatures has led researchers at Los Alamos National Laboratory to train bees for explosives detection, and trained bees are used in a handheld device by Inscentinel for the detection of explosives and other analytes.[12,13] The antennal-specific protein-1 (ASP1), an OBP from honeybee, *Apis mellifera*, contains a C-terminal tail fragment that has been shown to bind to pheromones and other chemical targets.[14] Four amino acids residues (Trp-Phe-Val-Ile) at the C-terminus end play an important role in binding to TNT.[15] Interestingly, the tetrapeptide sequence from ASP1 protein shares homology to the C-terminal end of the TNT binding dodecapeptide identified by Goldman *et al.* (Trp-His-Arg-Thr-Pro-Ser-Thr-Leu-Trp-Gly-Val-Ile) from a phage peptide library.[8] We fused the four amino acids to the C-terminal end of the P1 peptide *via* a tetraglycine linker to create a diblock P1ASP1C peptide (-His^1-Ser^2-Ser^3-Tyr^4-Trp^5-Tyr^6-Ala^7-Phe^8-Asn^9-Asn^{10}-Lys^{11}-Thr^{12}-Gly^{13}-Gly^{14}-Gly^{15}-Gly^{16}-Trp^{17}-Phe^{18}-Val^{19}-Ile^{20}). The P1ASP1C diblock peptide was then used to functionalize the surface of SWNTs in a FET device. In this study, we show the structural and functional properties of P1ASP1C upon adsorption onto SWNTs using computational modeling and experimental techniques and provide evidence for using designer peptides as recognition elements in the fabrication of a selective SWNT-FET chemosensor.

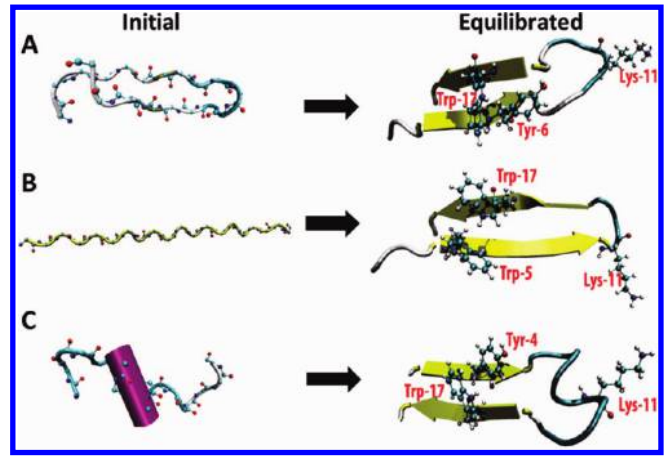

Figure 1. Peptide P1ASP1C structure prediction using molecular dynamics simulations. Starting three different initial conformations A, B, and C (left panels) and equilibrated structures (right panels). Interaction between Trp^{17}-Phe^{18} from one side and Tyr^4-Trp^6-Tyr^5 from the other side stabilizes the sheet structure, while the bulkiness of Asn^9-Asn^{10}-Lys^{11}-Thr^{12} destabilizes the helix structure.

RESULTS

The limiting factors in the use of biomolecules as sensing elements are their stability and orientation when interacting with the surface of a device. Therefore, when designing SWNT−biomolecule hybrids, it is critical to understand the effect of carbon nanotubes on the structure of the adsorbed biomolecules. It has been reported that the enzyme α-chymotrypsin undergoes substantial secondary structure changes upon adsorption onto SWNTs, resulting in complete loss of catalytic activity.[16] Smaller peptide sequences have also been shown to undergo a structural transition upon SWNT binding.[17,18] This has raised concerns about the structural and functional integrity of the adsorbed biomolecules on the SWNT surface.

To investigate the effect of SWNTs on the P1ASP1C peptide, we first obtained the structure of the peptide in its native and SWNT-bound states using circular dichriosm (CD) spectroscopy and computational modeling. The initial coordinates of P1ASP1C were predicted using Rosetta software.[19] Given the P1ASP1C sequence, 1289 structures were generated and clustered into five clusters. Top five energy-minimized structures were obtained using AMBER10. The structure with the lowest energy was further equilibrated using AMBER10 replica exchange molecular dynamics (REMD) simulations. The REMD consisted of 20 replicas with temperatures exponentially spaced between 270 and 700 K. Possible replica exchanges were tested every 1 ps, and 10 000 tests were done. Additional MD simulations were performed for the replica at 298.48 K to achieve saturated root mean square deviation (rmsd). The initial and equilibrated structures are shown in row A in Figure 1. Since no homological structure templates were found for P1ASP1C, we further tested the reliability of the Rosetta prediction using two different sets of initial P1ASP1C structures shown in rows B and C in Figure 1.

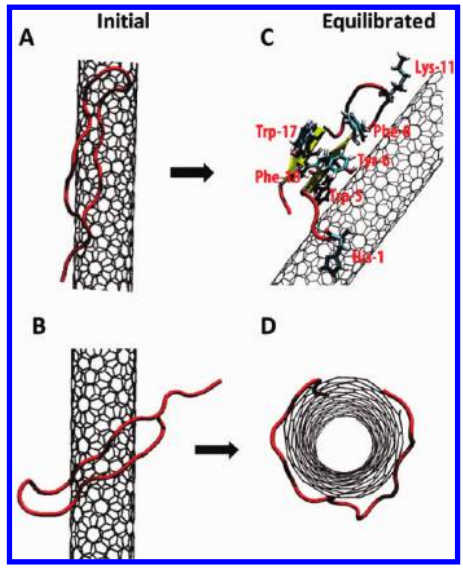

Figure 2. P1ASP1C peptide structure prediction in the presence of SWNT using molecular dynamics simulations. Starting with two different configurations A and B of the P1ASP1C−SWNT hybrid, we obtained two equilibrated configurations C and D. In C, the β-sheet structure is retained with Trp[5] playing an important role in the adsorption. In D, an unordered coil wraps around the nanotube.

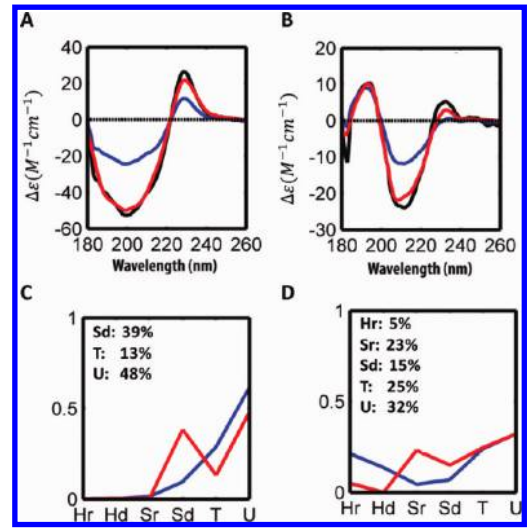

Figure 3. CD spectrum of (A) P1ASP1C in solution (black) and fitted using SELCON (blue) and CONTIN (red) and (B) P1ASP1C−SWNT in solution (black) and fitted using SELCON (blue) and CONTIN (red). (C) Secondary structure components extracted based on the fitting from (A). (D) Secondary structure components extracted based on the fitting in (B). The percentage of α-helix, β-sheet, β-turn, and random coil present obtained using the CONTIN method (inset).

The initial structure in row B is an extended β-strand. The initial structure in row C is made of the C-terminal part of ASP1. Starting with three different initial structures (Figure 1, left panels), molecular dynamics simulations were performed using different random seeds for each starting coordinates. The potential energy of the three equilibrated systems is about −400 kcal/mol (Figure 1, right panels). In all three cases, the final structures show that the hydrophobic groups Tyr[4]-Trp[5]-Tyr[6]-Ala[7]-Phe[8] from the N-terminal half and Trp[17]-Phe[18]-Val[19]-Ile[20] from the C-terminal half pack together to form β-sheets due to the hydrophobic interaction. The bulkiness of the adjacent four residues Asn[9]-Asn[10]-Lys[11]-Thr[12]- destabilizes an α-helix so that turns occur in that region. From a statistical point of view, they all converge into the same structure.

The equilibrated peptide predicted from Rosetta was subsequently placed above the SWNT in two different geometries, in which the peptide lies parallel or perpendicular to the axis of the SWNT, as shown in Figure 2A,B, respectively. For each initial P1ASP1C−SWNT structure, three independent MD runs were performed. Among the six total simulations, two equilibrated P1ASP1C−SWNT structures (Figure 2C,D) were obtained. We defined the structures in Figure 2C,D as folding and wrapping conformations, respectively. The dependence of the final biomolecular conformations on the initial configurations has also been observed in the MD simulations of a ssDNA−SWNT hybrid system.[20] A large-scale REMD simulation has revealed a rugged free energy landscape with multiple minima corresponding to distinct conformations.[21] Within typical MD time scales (10−100 ns), the system may be trapped in those metastable configurations. In addition, many simulation examples have shown that a native structure is not necessary corresponding to the global minimum energy state.[22,23] Therefore, to further determine the conformation of the P1ASP1C on the SWNT surface, we resorted to circular dichroism (CD) spectroscopy and atomic force microscopy (AFM) analyses.

CD and AFM Studies. Molecular dynamics simulations predicted that the main structural content of the P1ASP1C consists of β-sheet and turns with two possible conformations for P1ASP1C upon interaction with the carbon nanotube. The folding conformation almost retains the P1ASP1C structure, but the wrapping conformation is significantly different from the starting P1ASP1C predicted structure. CD and AFM scanning height analysis were performed and used to verify our computational results. The CD spectrum of P1ASP1C (0.2 mg/mL) in solution indicate an unordered structure (Figure 3A). When the SWNTs are dispersed in the presence of P1ASP1C peptide, we observed changes in the CD spectra. We used two different algorithms called SELCON and CONTIN for secondary structure determination.[24] The CD spectrum of P1ASP1C peptide was fitted into 10 different sets of known protein structures using SELCON and CONTIN. Secondary structures can be quantified by comparing the P1ASP1C spectrum to that of well-characterized protein structure. The SELCON and CONTIN algorithms quantify the percentage of α-helix, β-sheet, β-turn, and random coil present in the P1ASP1C before and after absorption onto the nanotube. The fitting of CD using SELCON and CONTIN is shown in Figure 3A,B for P1ASP1C and P1ASP1C−SWNT, respectively. The structural fractions, regular

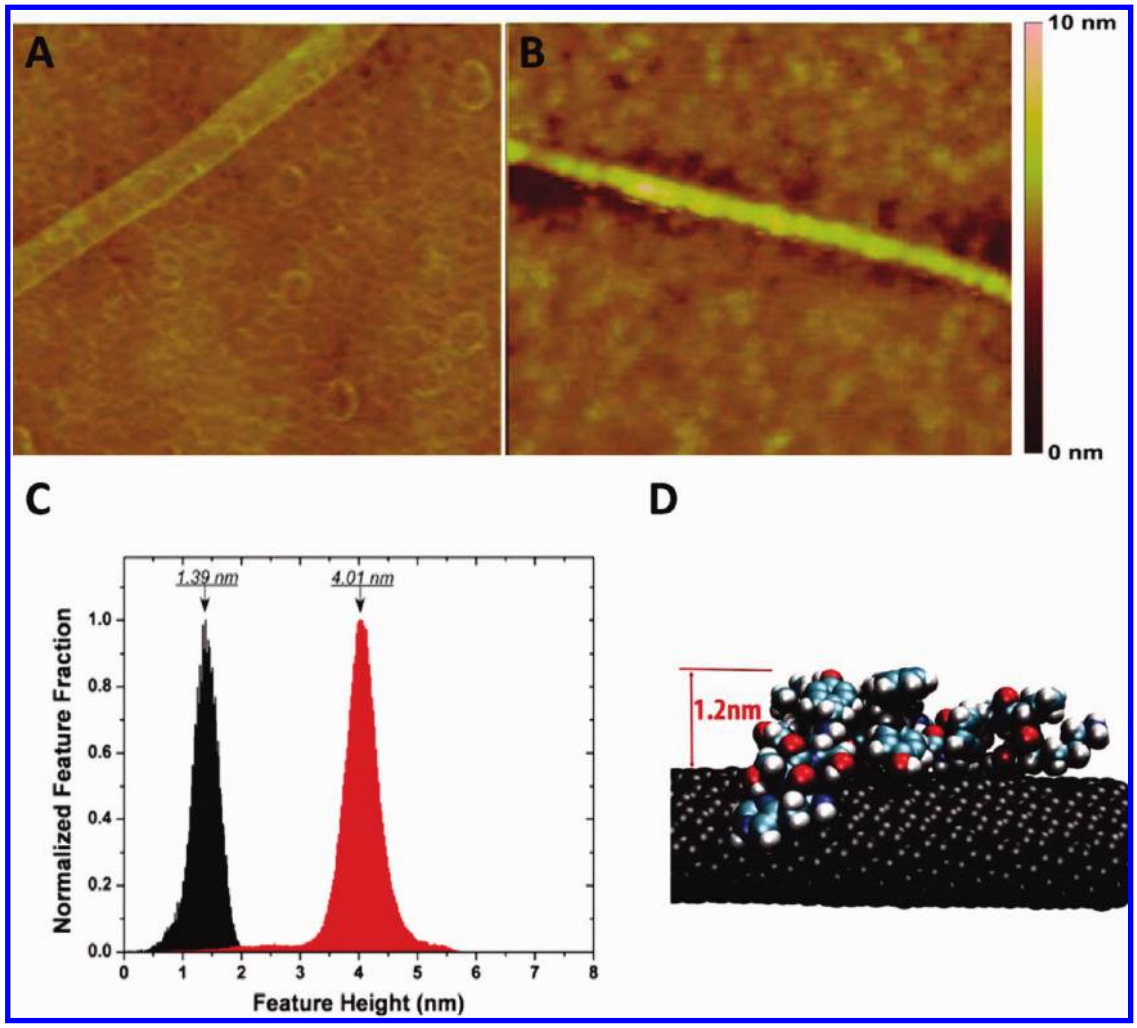

Figure 4. Adsorption of P1ASP1C peptide on nanotube. AFM topography images of 1.1 μm × 1.1 μm scan of (A) bare and (B) P1ASP1C-coated SWNTs. Note that the width of the SWNTs is larger than normal due to the AFM tip artifact. (C) Normalized feature-height histograms deduced from (A) SWNT and (B) P1ASP1C-adsorbed SWNT. (D) P1ASP1C−SWNT depicted from MD stimulation.

α-helix (Hr), distorted α-helix (Hd), regular β-sheet (Sr), distorted β-sheet (Sd), turns (T), and unordered coil (U), extracted from CONTIN are shown in Figure 3C,D. Both of the fitting models show that P1ASP1C reconfigures to more structured state by increasing α-helical and β-sheet fractions upon interaction with the carbon nanotube. Ramachandran histograms that are composed with 1000 equilibrated trajectory snapshots for P1ASP1C and P1ASP1C−SWNT show that the main structural fractions of P1ASP1C peptide are in the β-sheet region and restructure into more ordered configuration when adsorbed onto the SWNT by increasing the β-sheet fraction (data not shown). The numerical percentages of each structural component deducted from CONTIN method are in good agreement the Ramachandran histogram, implying that P1ASP1C predominantly retains β-sheet conformation upon its adsorption onto the SWNT. The P1ASP1C peptide coating on CNTs was also analyzed by AFM to confirm the adsorption of the P1ASP1C peptide onto the carbon nanotube. As shown in Figure 4, a topological difference between a bare SWNT and P1ASP1C-coated nanotube can be observed. The P1ASP1C peptide was found to uniformly coat the carbon nanotube. In Figure 4C, the feature height histogram in the AFM scans shows that the bare nanotube has a diameter of 1.4(±0.25) nm, and upon adsorption of the P1ASP1C peptide, the height scan increased to 4.05(±0.32) nm. From these, the thickness of the peptide coating around the nanotube is estimated to ~2.6 nm. This calculated thickness is comparable to the computed peptide thickness of 1.2 or 2.4 nm for complete coating around the nanotube (Figure 4D). It is well-known that aromatic amino acids such as in phenylalanine (Phe), tryptophan (Trp), and tyrosine (Tyr) can bind to SWNTs *via* π−π interactions.[25,26] The amino acid Trp[5] plays an important role in binding to SWNT through π−π stacking, as shown in Figure 2. Substitution of Trp[5] with alanine reduced its interaction with the carbon nanotube. This is not surprising because other studies have also indicated the importance of tryptophan in SWNT binding.[26] Therefore, on the basis of CD and AFM analyses, the predicted fold-

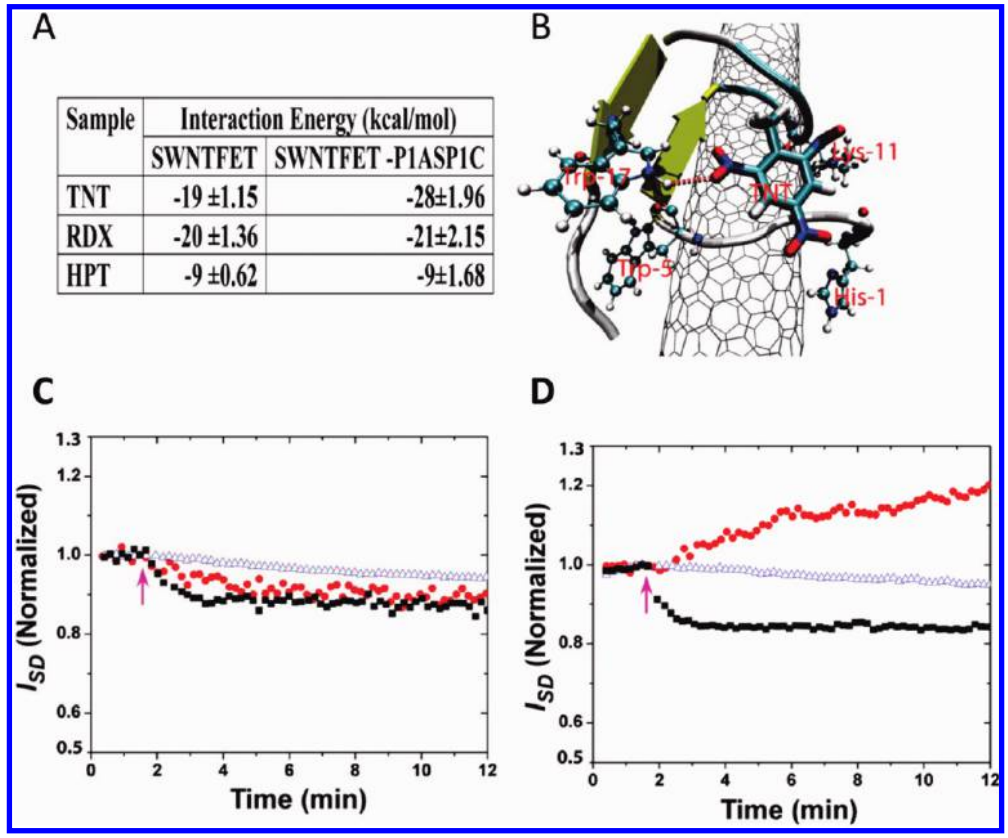

Sample	Interaction Energy (kcal/mol)	
	SWNTFET	SWNTFET -P1ASP1C
TNT	-19 ±1.15	-28±1.96
RDX	-20 ±1.36	-21±2.15
HPT	-9 ±0.62	-9±1.68

Figure 5. (A) Interaction energy of TNT, RDX, and HPT with bare SWNT or P1ASP1C-decorated SWNT. (B) Computational modeling predicts that TNT binds to P1ASP1C−SWNT hybrid through a H bond with Trp[17] and π−π interaction with the SWNT surface. Response of (C) bare SWNT-FET and (D) P1ASP1C-coated SWNT-FET to TNT (red circles), RDX (blue triangles), and HPT (black squares). Arrow indicates when the vapor was introduced into the device. Note that the chemical agents were exposed under ambient conditions.

ing of P1ASP1C on the nanotube is reliable and can be used for further theoretical molecular binding studies as described below.

P1ASP1C−SWNT As a Chemical Sensor. Using the equilibrated structures shown in Figure 2C, we calculated the interaction energy between P1ASP1C−SWNT and three different chemical agents 2,4,6-trinitrotoluene (TNT), cyclotrimethylenetrinitramine (RDX), and 2-heptanone (HPT) using MD simulations. Docking TNT, RDX, and HPT onto different positions above P1ASP1C−SWNT using AutoDock program, we performed MD simulations to generate equilibrated trajectories of the system. In several trials, RDX and HPT migrate away from the peptide to the surface of SWNT so that the calculated interaction energy of RDX and HPT with the bare SWNT and P1ASP1C−SWNT remains similar, as shown in Figure 5A. However, the nitro group of TNT forms a hydrogen bond with Trp[17], while the ring of TNT stacks on the surface of the SWNT, as shown in Figure 5B. This provides a binding motif for TNT to the P1ASP1C−SWNT hybrid, where their interaction energy is calculated to be ~9 kcal/mol lower than that of TNT with a bare nanotube (Figure 5A). Previous studies have also shown the importance of amino acid tryptophan for the proteins binding to TNT.[27−29] Experimentally, P1ASP1C showed a strong affinity for TNT with a K_D of ~36 nM as determined by surface plasmon resonance using a Biacore surface lasmon resonance system. Since the intrinsic density of states of a SWNT is extremely sensitive to its physiochemical environment, binding of TNT to P1ASP1C−SWNT should affect the electronic properties of the nanotube. We tested the ability of a SWNT-FET device coated with the P1ASP1C peptide, which could serve as a recognition element, to detect TNT. The SWNT-FET device was fabricated and decorated with P1ASP1C peptide. The SWNT-FET device effectively serves to function as a transduction device that mimics the signal transduction process seen in biology.

The SWNT-FET was exposed to TNT, RDX, and HPT vapors as described in the Methods section. While these chemicals have similar molecular weights, the variation in the vapor concentration is due to differences in the vapor pressure (P) at the given experimental condition (*e.g.*, $P^{RDX} = 5 \times 10^{-9}$ Torr, $P^{TNT} = 9 \times 10^{-6}$ Torr, and $P^{HPT} = 1.6$ Torr at 25 °C, 1 atm). Moreover, the extremely low P and the wide variation in thermal desorption of explosive chemicals hinder one from forming equivalent vapor concentration for each agent. Thus, for the sake of experimental access, the selectivity of a PRE-decorated SWNT-FET was probed by comparing its

response with bare SWNT-FET responses for a given chemical vapor. The sensing of TNT by the P1ASP1C peptide-coated and -uncoated SWNT-FET device was investigated by monitoring the source−drain current (I_{SD}). The circuit characteristics of a bare SWNT-FET and P1ASP1C-functionalized SWNT-FET device are shown in Figure 5C,D, respectively. The P1ASP1C-functionalized SWNT-FET exhibits selective response to TNT by showing that I_{SD} increases upon exposure to TNT, while bare SWNT-FET responds by decreasing its I_{SD}. The exposure to RDX and HPT vapors shows no such selectivity by showing changes in the I_{SD} characteristics that were similar in both the bare SWNT-FET and P1ASP1C-functionalized SWNT-FET device. Therefore, P1ASP1C-decorated SWNT-FET showed maximal distinct changes to TNT vapors. As a control, we also tested a SWNT-FET device coated with a P1R5 peptide and observed no selectivity in the I_{SD} when exposed to TNT vapors. Therefore, the ASP1 tetrapeptide domain dictates the specific recognition toward TNT vapors. Interestingly, HPT, an insect pheromone, elicited similar responses from both the bare SWNT-FET and P1ASP1C-functionalized SWNT-FET device, while vapors of RDX, another explosive chemical, caused no changes in the I_{SD} behavior. This elucidates the discriminating property of the peptide-coated FET device because HPT and RDX do not effectively interact with the P1ASP1C-coated SWNT-FET device. Moreover, the noncovalent nature of binding between TNT molecules and P1ASP1C peptide enables one to recover and recycle the PRE-functionalized SWNT-FET sensor. Here, vacuum drying at ambient temperature for a few minutes accelerates the return to its active state. When the P1ASP1C-coated SWNT-FET device was tested in liquid-gated sensor configuration, parts per trillion levels of TNT were detected in an aqueous environment.

In conclusion, we designed a PRE that can spontaneously decorate SWNTs and provide target selectivity in a FET-based chemical sensor. This approach can be used to fabricate SWNT-FET devices that could be optimized to detect traces of specific targets using PREs. Additionally, nucleic acid based aptamer recognition elements (AREs) can be used as an alternative approach to design selective chemical sensors.

METHODS

Computational Methods. We first studied the adsorption of P1ASP1C (ligand) onto SWNT (substrate) and the interaction between P1ASP1C-SWNT hybrid and chemical analytes such as TNT, cyclotrimethylenetrinitramine (RDX), and 2-heptanone (HPT) (a natural ligand) using classical all-atom molecular dynamics simulations. The initial coordinates of a SWNT with chirality of (11,3) and length of 8 nm were generated using Shigeo Maruyama's wrapping program (http://www.photon.t.u-tokyo.ac.jp/~maruyama/wrapping3/wrapping.html). The SWNT atoms were modeled as uncharged Lennard-Jones particles using sp^2-type carbons in AMBER99SB force field. The peptide was also modeled using AMBER99SB force field.[30] The GB5 model was used to model solvent effect. Chloride ions were used to neutralize all of the systems. The structure of studied chemical analytes TNT, RDX, and HPT was built using InsightII and optimized using HF/6-31G** in Gaussian 03.[31] AMBER general force field was used to model the compounds.

First, all of the systems were equilibrated until the root-mean-square deviation (rmsd) of the backbone atoms was saturated. Then, additional 200 ps MD simulations were performed to collect trajectory snapshots every 2 ps for energy calculations. To estimate the relative binding affinity of ligands to substrates, the interaction energy $\Delta E_{interact}$ was calculated in vacuum phase since the experiments were performed under vapor conditions. The interaction energy is defined as the difference of total potential energy before and after binding, where E_{bond}, E_{angle}, $E_{torsion}$, E_{vdw}, and E_{ele} are the bond stretching, the angle bending, the torsion, the van der Waals interaction, and the electrostatic energy, respectively.

$$\Delta E_{interact} = E(\text{complex}) - E(\text{ligand}) - E(\text{substrate}) \quad (1)$$

$$E = E_{bond} + E_{angle} + E_{torsion} + E_{vdw} + E_{ele} \quad (2)$$

Experimental Methods. The termini-unblocked P1ASP1C peptide was synthesized by New England Peptide (Gardner, MA). Si wafers with 1 μm thermal oxide were purchased from University Wafers (South Boston, MA). A monolayer of networked SWNTs was CVD grown on the Si wafer using previously published procedures.[32,33] Nanoparticles of iron hydroxide were deposited on the thermal oxide layer by immersing the wafer in an aqueous solution of 10 μM iron hydroxide hexahydrate for 10 s. The catalyst was oxidized by exposing the wafer to air at 800 °C. The air was exchanged with 250 sccm Ar flow for 5 min, and 500 sccm of H_2 was introduced while heating up to 830 °C. Ar flow was replaced with 250 sccm of CH_4 and 250 sccm of H_2, while the temperature was raised to 900 °C. The nanotube growth was terminated after 20 min by switching the CH_4 and H_2 gases to 150 sccm of Ar until the growth oven cooled down to room temperature. The density of SWNTs was controlled by adjusting the concentration of catalyst particles. Conventional microlithography was introduced to pattern 30/80 nm thick Cr/Au layer on both sides of electrodes for the gate, source, and drain electrodes. Peptides were dissolved in deionized water at the concentration of 0.2 mg/mL. Two microliters of the peptide solutions was dropped on the SWNT channel and incubated for 15 min in a 100% humidity chamber. The peptide-loaded SWNT-FET was extensively washed with deionized water and dried. The SWNT-FET device functionalized with P1ASP1C peptide was exposed to the chemical agents by introducing the vapors directly onto the device surface. A MMR 4-probe station equipped with a Keithley semiconductor parameter analyzer (SCS4200) was used to characterize the SWNT-FET device performance in various sensing environments. SWNT-FET source−drain current was monitored at gate and source−drain bias voltage of −0.5 and 0.2 V, respectively, while exposed to various chemical vapors. The SWNT-FET devices were exposed to TNT (12 ppb), RDX (6.6 ppt), and HPT (2100 ppm) vapors in the chamber saturated with each vapor at 25 °C 1 atm. Topographic images of the SWNT channels were taken using a Digital Instruments nanoscope IV-multimode AFM in noncontacting mode. Binding of P1ASP1C to TNT was also determined by surface plasmon resonance using a Biacore system. P1ASP1C was immobilized onto a CM5 chip using EDC/NHS coupling and blocked with ethanolamine. TNT dilutions were made in 10 mM HEPES buffer, 150 mM sodium chloride, 3 mM EDTA, and 0.05% surfactant P20.

Acknowledgment. We would like to thank R. Patcher for useful discussion, X. Duan and R. Berry for the supercomputer support, M. Tomczak for CD analysis, and J. Slocik for SPR measurements. This research was performed while S.K. held a National Research Council Research Associateship Award at AFRL. This work was funded by AFOSR and AFRL/RX.

REFERENCES AND NOTES

1. Kong, J.; Franklin, N. R.; Zhou, C.; Chapline, M. G.; Peng, S.; Cho, K.; Dai, H. Nanotube Molecular Wires as Chemical Sensors. *Science* **2000**, *287*, 622–625.
2. Romero, H. E.; Bolton, K.; Rosen, A.; Eklund, P. C. Atom Collision-Induced Resistivity of Carbon Nanotubes. *Science* **2005**, *307*, 89–93.
3. Forzani, E. S.; Li, X.; Zhang, P.; Tao, N.; Zhang, R.; Amlani, I.; Tsui, R.; Nagahara, L. A. Tuning the Chemical Selectivity of SWNT-FETs for Detection of Heavy-Metal Ions. *Small* **2006**, *2*, 1283–1291.
4. So, H. M.; Won, K.; Kim, Y. H.; Kim, B. K.; Ryu, B. H.; Na, P. S.; Kim, H.; Lee, J. O. Single-Walled Carbon Nanotube Biosensors using Aptamers as Molecular Recognition Elements. *J. Am. Chem. Soc.* **2005**, *127*, 11906–11907.
5. McAlpine, M. C.; Agnew, H. D.; Rohde, R. D.; Blanco, M.; Ahmad, H.; Stuparu, A. D.; Goddard, W. A.; Heath, J. R. Peptide−Nanowire Hybrid Materials for Selective Sensing of Small Molecules. *J. Am. Chem. Soc.* **2008**, *130*, 9583–9589.
6. Sarikaya, M.; Tamerler, C.; Jen, A. K.; Schulten, K.; Baneyx, F. Molecular Biomimetics: Nanotechnology through Biology. *Nat. Mater.* **2003**, *2*, 577–585.
7. Pender, M. J.; Sowards, L. A.; Hartgerink, J. D.; Stone, M. O.; Naik, R. R. Peptide-Mediated Formation of Single-Wall Carbon Nanotube Composites. *Nano Lett.* **2006**, *6*, 40–44.
8. Goldman, E. R.; Pazirandeh, M. P.; Charles, P. T.; Balighian, E. D.; Anderson, G. P. Selection of Phage Displayed Peptides for the Detection of 2,4,6-Trinitrotoluene in Seawater. *Anal. Chim. Acta* **2002**, *457*, 13–19.
9. Kroger, N.; Deutzmann, R.; Sumper, M. Polycationic Peptides from Diatom Biosilica that Direct Silica Nanosphere Formation. *Science* **1999**, *286*, 1129–1132.
10. Danty, E.; Briand, L.; Michard-Vanhee, C.; Perez, V.; Arnold, G.; Gaudemer, O.; Huet, D.; Huet, J. C.; Ouali, C.; Masson, C.; Pernollet, J. C. Cloning and Expression of a Queen Pheromone-Binding Protein in the Honeybee: An Olfactory-Specific, Developmentally Regulated Protein. *J. Neurosci.* **1999**, *19*, 7468–7475.
11. Lartigue, A.; Gruez, A.; Briand, L.; Blon, F.; Bezirard, V.; Walsh, M.; Pernollet, J. C.; Tegoni, M.; Cambillau, C. Sulfur Single-Wavelength Anomalous Diffraction Crystal Structure of a Pheromone-Binding Protein from the Honeybee *Apis mellifera* L. *J. Biol. Chem.* **2004**, *279*, 4459–4464.
12. Mead, J. C. *New Scientist* **2007**, November issue.
13. Inscentinel Ltd, U.K. (www.inscentinel.com).
14. Pesenti, M. E.; Spinelli, S.; Bezirard, V.; Briand, L.; Pernollet, J. C.; Tegoni, M.; Cambillau, C. Structural Basis of the Honey Bee PBP Pheromone and pH-Induced Conformational Change. *J. Mol. Biol.* **2008**, *380*, 158–169.
15. Kuang, Z.; Naik, R. R.; Farmer, L. B. To be submitted.
16. Karajanagi, S. S.; Vertegel, A. A.; Kane, R. S.; Dordick, J. S. Structure and Function of Enzymes Adsorbed onto Single-Walled Carbon Nanotubes. *Langmuir* **2004**, *20*, 11594–11599.
17. Zheng, L.; Jain, D.; Burke, P. Nanotube−Peptide Interactions on a Silicon Chip. *J. Phys. Chem. C* **2009**, *113*, 3978–3985.
18. Dieckmann, G. R.; Dalton, A. B.; Johnson, P. A.; Razal, J.; Chen, J.; Giordano, G. M.; Munoz, E.; Musselman, I. H.; Baughman, R. H.; Draper, R. K. Controlled Assembly of Carbon Nanotubes by Designed Amphiphilic Peptide Helices. *J. Am. Chem. Soc.* **2003**, *125*, 1770–1777.
19. Rohl, C. A.; Strauss, C. E.; Misura, K. M.; Baker, D. Protein Structure Prediction Using Rosetta. *Methods Enzymol.* **2004**, *383*, 66–93.
20. Johnson, R. R.; Johnson, A. T.; Klein, M. L. Probing the Structure of DNA−Carbon Nanotube Hybrids with Molecular Dynamics. *Nano Lett.* **2008**, *8*, 69–75.
21. Johnson, R. R.; Kohlmeyer, A.; Johnson, A. T.; Klein, M. L. Free Energy Landscape of a DNA−Carbon Nanotube Hybrid Using Replica Exchange Molecular Dynamics. *Nano Lett.* **2009**, *9*, 537–541.
22. Liwo, A.; Khalili, M.; Scheraga, H. A. *Ab Initio* Simulations of Protein-Folding Pathways by Molecular Dynamics with the United-Residue Model of Polypeptide Chains. *Proc. Natl. Acad. Sci. U.S.A.* **2005**, *102*, 2362–2367.
23. Skolnick, J. Putting the Pathway Back into Protein Folding. *Proc. Natl. Acad. Sci. U.S.A.* **2005**, *102*, 2265–2266.
24. Sreerama, N.; Venyaminov, S. Y.; Woody, R. W. Estimation of Protein Secondary Structure from Circular Dichroism Spectra: Inclusion of Denatured Proteins with Native Proteins in the Analysis. *Anal. Biochem.* **2000**, *287*, 243–251.
25. Zorbas, V.; Smith, A. L.; Xie, H.; Ortiz-Acevedo, A.; Dalton, A. B.; Dieckmann, G. R.; Draper, R. K.; Baughman, R. H.; Musselman, I. H. Importance of Aromatic Content for Peptide/Single-Walled Carbon Nanotube Interactions. *J. Am. Chem. Soc.* **2005**, *127*, 12323–12328.
26. Li, X.; Chen, W.; Zhan, Q.; Dai, L.; Sowards, L.; Pender, M.; Naik, R. R. Direct Measurements of Interactions between Polypeptides and Carbon Nanotubes. *J. Phys. Chem. B* **2006**, *110*, 12621–12625.
27. Little, J. R.; Eisen, H. N. Evidence for Tryptophan in the Active Sites of Antibodies to Polynitrobenzenes. *Biochemistry* **1967**, *6*, 3119–3125.
28. Jaworski, J. W.; Raorane, D.; Huh, J. H.; Majumdar, A.; Lee, S. W. Evolutionary Screening of Biomimetic Coatings for Selective Detection of Explosives. *Langmuir* **2008**, *24*, 4938–4943.
29. Khan, H.; Barna, T.; Harris, R. J.; Bruce, N. C.; Barsukov, I.; Munro, A. W.; Moody, P. C.; Scrutton, N. S. Atomic Resolution Structures and Solution Behavior of Enzyme−Substrate Complexes of *Enterobacter cloacae* PB2 Pentaerythritol Tetranitrate Reductase: Multiple Conformational States and Implications for the Mechanism of Nitroaromatic Explosive Degradation. *J. Biol. Chem.* **2004**, *279*, 30563–30572.
30. Cornell, C. N.; Sigman, M. S. Discovery of and Mechanistic Insight into a Ligand-Modulated Palladium-Catalyzed Wacker Oxidation of Styrenes Using TBHP. *J. Am. Chem. Soc.* **2005**, *127*, 2796–2797.
31. Frisch, M.; Trucks, G. W.; Schlegel, H. B.; Scuseria, G. E.; Robb, M. A.; Cheeseman, J. R.; Montgomery, J. A., Jr.; Vreven, T.; Kudin, K. N.; Burant, J. C.; Millam, J. M.; Iyengar, S. S.; Tomasi, J.; Barone, V.; Mennucci, B.; Cossi, M.; Scalmani, G.; Rega, N.; Petersson, G. A.; Nakatsuji, H.; Hada, M.; Ehara, M.; Toyota, K.; Fukuda, R.; Hasegawa, J.; Ishida, M.; Nakajima, T.; Honda, Y.; Kitao, O.; Nakai, H.; Klene, M.; Knox, J. E.; Hratchian, H. P.; Cross, J. B.; Bakken, V.; Adamo, C.; Jaramillo, J.; Gomperts, R.; Stratmann, R. E.; Yazyev, O.; Austin, A. J.; Cammi, R.; Pomelli, C.; Ochterski, J. W.; Ayala, P. Y.; Morokuma, K.; Voth, G. A.; Salvador, P.; Dannenberg, J. J.; Zakrzewski, V. G.; Dapprich, S.; Daniels, A. D.; Strain, M. C.; Farkas, O.; Malick, D. K.; Rabuck, A. D.; Raghavachari, K.; Foresman, J. B.; Ortiz, J. V.; Cui, Q.; Baboul, A. G.; Clifford, S.; Cioslowski, J.; Stefanov, B. B.; Liu, G.; Liashenko, A.; Piskorz, P.; Komaromi, I.; Martin, R. L.; Fox, D. J.; Keith, T.; Al-Laham, M. A.; Peng, C. Y.; Nanayakkara, A.; Challacombe, M.; Gill, P. M. W.; Johnson, B.; Chen, W.; Wong, M. W.; Gonzalez, C.; Pople, J. A. *Gaussian 03*; Gaussian, Inc.: Wallingford, CT, 2004.
32. Chen, R. J.; Choi, H. C.; Bangsaruntip, S.; Yenilmez, E.; Tang, X.; Wang, Q.; Chang, Y. L.; Dai, H. An Investigation of the Mechanisms of Electronic Sensing of Protein Adsorption on Carbon Nanotube Devices. *J. Am. Chem. Soc.* **2004**, *126*, 1563–1568.
33. Kramer, R. M.; Sowards, L. A.; Pender, M. J.; Stone, M. O.; Naik, R. R. Constrained Iron Catalysts for Single-Walled Carbon Nanotube Growth. *Langmuir* **2005**, *21*, 8466–8470.